

Role of Four-Fold Coordinated Titanium and Quantum Confinement in CO₂ Reduction at Titania Surface

Donghwa Lee and Yosuke Kanai*

Condensed Matter and Materials Division, Lawrence Livermore National Laboratory, Department of Chemistry, The University of North Carolina, Chapel Hill, North Carolina, United States

S Supporting Information

ABSTRACT: Photocatalytic reduction of carbon dioxide (CO₂) into hydrocarbons is an attractive approach for mitigating CO₂ emission and generating useful fuels at the same time. Titania (TiO₂) is one of the most promising photocatalysts for this purpose, and nanostructured TiO₂ materials often lead to an increased efficiency for the photocatalytic reactions. However, what aspects of and how such nanomaterials play the important role in the improved efficiency are yet to be understood. Using first-principles calculations, reaction mechanisms on the surface of bulk anatase TiO₂(101) and of a small TiO₂ nanocluster were investigated to elucidate the role of four-fold coordinated titanium atoms and quantum confinement (QC) in the CO₂ reduction. Significant barrier reduction observed on the nanocluster surface is discussed in terms of how the under-coordinated titanium atoms and QC influence CO₂ reduction kinetics at surface. It is shown that the reduction to CO can be greatly facilitated by the under-coordinated titanium atoms, and they also make CO₂ anion formation favorable at surfaces.

Ever since photolysis was observed on semiconductor surfaces by Honda and Fujishima in 1972,¹ the field has attracted considerable attention.² Photocatalytic conversion of water molecules to hydrogen and oxygen molecules has been extensively investigated ever since.³ The seminal work on CO₂ reduction on several semiconductor surfaces in 1979 by Inoue et al.⁴ indicated another exciting prospect and has prompted various aspects of the promising TiO₂ to be investigated for improving the photocatalytic activity and selectivity.⁵ While the enhanced photocatalytic activity has been reported using metal cocatalysts and/or through tailoring TiO₂ itself,^{6,7} detailed photocatalytic CO₂ reduction mechanism is not well understood. There are even some recent studies calling for more systematic analysis of the reduction process because the conventional view does not appear to hold⁸ and also the product selectivity (CH₄, CH₃OH, HCO₂H, CO, etc.) appears to depend significantly on atomistic details.⁹

Obtaining physical insights into the enhanced reactivity associated with nanomaterials is very much needed for clarifying the reduction mechanism and for improving the efficiency. However, what and how specific material features are responsible for the improved reactivity have not been determined. Many have proposed that the increased number of unsaturated four-fold coordinated titanium atom (Ti₄) sites,

which are widely present on TiO₂ nanomaterials surfaces, is an important factor.¹⁰ At the same time, presence of the surface Ti₄ sites on anatase surface itself is still an open question.^{11–14} Importance of the conduction band position has also been proposed to account for the efficient photocatalytic conversion, suggesting that a high conduction band position increases the reducing potential of photoexcited electrons at the TiO₂ surface,^{15–17} while others have proposed that the improved photocatalytic activity was related to the charge carrier mobility.^{18,19} Understanding how specific material characteristics of TiO₂ nanomaterials are playing the important role is crucial because the photocatalytic efficiency and product selectivity remains quite low even though significant progress has been made in recent years.¹⁷

First-principles calculations have previously identified several CO₂ adsorption sites on the predominant anatase TiO₂ (101) surface and on nanoclusters.^{20–22} However, CO₂ reduction mechanisms have not been investigated in regard to how nanomaterials make the reactions favorable. CO₂ conversion process into methane/methanol takes multiple reaction steps involving eight electrons and protons.²³ Here, we focus on the key initial steps of CO₂ reduction to HCOOH (formic acid) and CO (carbon monoxide), the “intermediate” species that lead to the final products.^{23,24} Note that Inoue et al. in 1979 proposed that both methane and methanol derive from HCOOH formation.⁴ We obtained detailed insights into what aspects of TiO₂ nanomaterials are important for the key CO₂ reduction step using first-principles electronic structure calculations.

From a chemical standpoint, reactions require two excess electrons to form either HCOOH or CO at the surface. We also considered reaction energetics for the systems with no and one excess electron, leading to extremely endothermic processes that cannot possibly occur in experiments (see Supporting Information, SI). Excess electrons are assumed to be already at the conduction band minimum prior to chemical reactions because of the significant difference in the relevant time scale of the two processes.²⁵ Protons are widely available from dissociation of water molecules at surface.²⁶ We employ DFT calculations²⁷ to investigate the key CO₂ reduction steps proposed in the literature (see SI for computational details).^{23,24}

Figure 1 shows TiO₂ structures used in our calculations. A (4×2) double dilayer slab model is used to represent the bulk

Received: October 5, 2012

Published: November 26, 2012

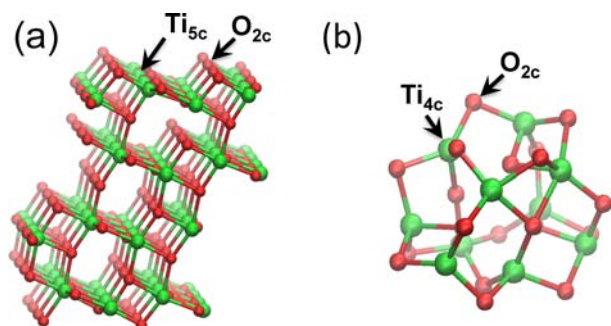


Figure 1. Structures of (a) TiO₂ anatase bulk surface and (b) QD used in our calculations. Titanium atoms at the bulk surface are five-fold coordinated, while the titanium atoms on the QD surface are four-fold coordinated.

surface of anatase (101). In addition to the bulk (101) anatase surface, a small quantum dot (QD) (~1 nm in diameter) as prepared in ref 28 was investigated to assess how a prototypical TiO₂ nanomaterial might exhibit unique reaction energetics. QD is characterized by an abundance of Ti₄ atoms at the surface and a quantum confinement (QC) effect,²⁹ and both have been proposed as being responsible for enhanced CO₂ reactivity in the literature.

We summarized our calculation results in Table 1 and Figure 2. Reduction mechanism to HCOOH is a two-step process.^{24,30}

Table 1. Reaction Energetics for Three CO₂ Reduction Mechanisms^a: (1) CO₂+H⁺+2e⁻→HCOO⁻; (2) CO₂+H⁺+2e⁻→CO+O⁻+H(CO+OH⁻); (3) CO₂+2e⁻→CO+O²⁻

product		first		second	
		E _a	E _f	E _a	E _f
HCOOH	bulk	1.20	-0.27	0.54	-0.06
	QD	0.60	-1.68	0.59	0.29
CO+OH	bulk	1.20	1.10	0.24	-0.66
	QD	0.60	-0.31	0.21	-0.27
CO+O	bulk	2.13	1.45	—	—
	QD	0.23	0.02	0.35	-0.29

^aE_a is the activation barrier for the reaction, and E_f is the reaction energy (see also Figure 2).

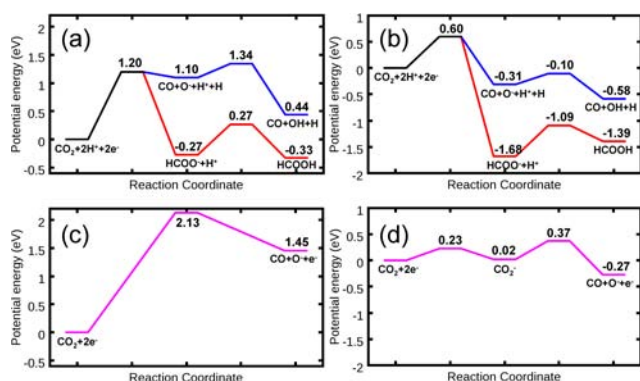


Figure 2. Potential energy profile along different reaction pathways: red line, HCOOH formation; blue line, CO formation with protons; and purple line, CO formation without protons. (a,c) Reaction energetics on the bulk surface and (b,d) QD surface.

First, a physisorbed CO₂ molecule reacts associatively with a hydrogen atom and an electron at the TiO₂ surface, forming a formate ion (HCOO⁻). Then, adsorbed HCOO⁻ abstracts a proton at the surface to form HCOOH. Our calculations show that the rate-determining step is the first step with a significant energy barrier of ~1.20 eV, while the overall reaction is slightly exothermic by 0.33 eV on the bulk surface (Figure 2a). On the other hand, the rate-determining energy barrier on the QD surface is only 0.60 eV, and the reaction is highly exothermic by 1.68 eV (Figure 2b). The alternative CO₂ reduction mechanism to CO also encounters a significant energy barrier of 1.20 eV on the bulk surface, while the barrier is only 0.60 eV for the QD surface. Interestingly, these rate-determining transition states (TS) for HCOO⁻ and CO formation are geometrically the same, but the TS leads to two distinct energy minima (Figure 3a,b); the energy landscape at the TS is indeed “monkey saddle” in character.³¹

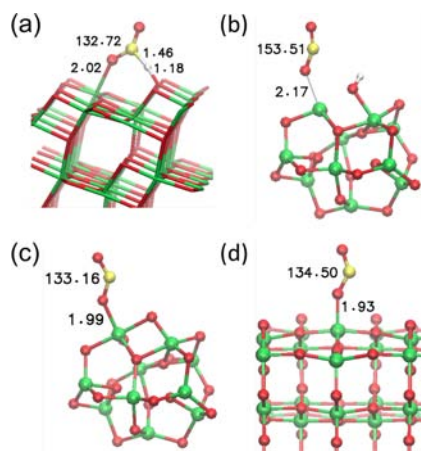


Figure 3. Geometries of CO₂ at monkey saddle point on (a) bulk and (b) QD surfaces. Geometries of CO₂⁻ metastable state (c) on the QD surface and (d) at four-fold coordinated Ti atom (Ti₄) on bulk surface with an oxygen vacancy.

Note that the TS on the bulk surface differs from that on the QD surface geometrically. Once CO is formed at the surface, the remaining oxygen and a proton at the surface could form a hydroxyl group with a small energy barrier (~0.2 eV) on both bulk and QD surfaces. Key structures of the reaction processes are summarized in Figures S6 and S7.

Comparison of projected density of electronic states (PDOS) for the initial physisorbed CO₂, resulting HCOO⁻, and CO at the bulk TiO₂ surface is shown in Figure 4. Conduction band minimum (CBM) of the bulk TiO₂ is located lower than CO₂ LUMO as expected. With HCOO⁻ formation at the surface, excess electrons in TiO₂ are transferred to the adsorbate because the resulting LUMO molecular state is formed within the TiO₂ energy gap. On the other hand, CO formation does not result in the electron migration from the TiO₂ surface to the molecule because the LUMO of CO is located much higher in energy than the TiO₂ CBM.

In addition to the two reaction mechanisms leading to HCOOH (through HCOO⁻) and CO formation, a simple electron-induced CO formation reaction was recently observed experimentally at a TiO₂ surface using STM.³² On the bulk surface without the presence of protons, our calculations show that this reaction mechanism is highly endothermic by 1.45 eV with a significant barrier of 2.13 eV (Figure 2c). It is thus

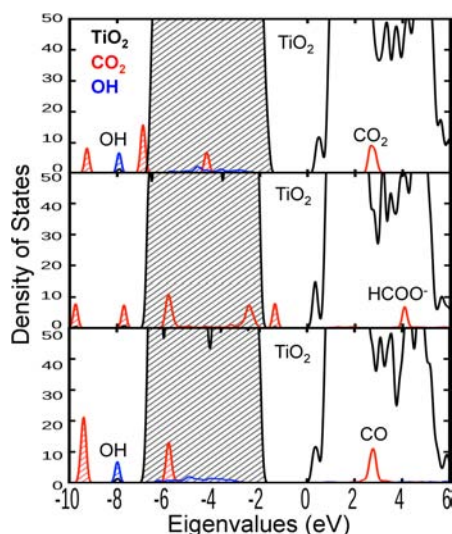


Figure 4. PDOS comparison of CO₂ (top), HCOO⁻ (middle), and CO (bottom). Excess electrons are on HCOO⁻, while they remain at the conduction band edge of TiO₂ for CO molecule.

evident that the presence of protons makes the reaction energetics highly favorable for CO formation. On the QD surface, this CO formation reaction is exothermic by 0.27 eV, and the rate-determining energy barrier is only 0.37 eV (Figure 2d), showing a quite different behavior from the bulk surface. Apparently, the difference comes from the formation of intermediate anion state (CO₂⁻) with the bending angle of 133° on the QD surface (Figure 3c). The Ti–O bond distance between the surface and the anion is 1.99 Å, which is only slightly larger than the Ti–O bond length (1.82–1.92 Å) in the TiO₂ QD itself, indicating significant interaction with the surface. This anion configuration was found to be energetically unstable at the bulk surface.

These results point to the important role of the Ti₄ and/or the QC effect for reducing the energy barrier in all three reaction mechanisms. In order to elucidate their role for each reaction mechanism, we investigate the rate-determining reaction step under two additional conditions. For investigating the role of the Ti₄, the bulk surface with an oxygen vacancy was created so that there are two Ti₄ sites at surface. For elucidating the role of the QC, a thin TiO₂ ribbon, which is periodic only in one direction, is used (see Figure S10). Figure 5a,c,e shows how the potential energy profile along the reaction coordinate changes with the presence of the Ti₄ atoms at the bulk surface for the rate-determining step of the three reaction mechanisms. All reactions show a very small energy barrier. For CO formation mechanisms, the intermediate CO₂⁻ state is formed prior to the CO formation. More advanced DFT calculations with Hubbard correction were performed for validating that this qualitative behavior is correct (see SI). The QC effect role was considered next with the TiO₂ ribbon. For HCOO⁻ formation, the barrier is significantly reduced to 0.41 eV, as seen in Figure 5b. For the two CO formation reactions, however, the QC does not change the energetics: the barrier remains high, and the reaction remains significantly endothermic (Figure 5d,f). Rather, CO formation reactions are more closely related to the ease of C–O bond dissociation facilitated by the formation of CO₂⁻ bound at the Ti₄ sites.

For HCOOH formation mechanism, relative stability between HCOO⁻ and HCOOH at surface is another important

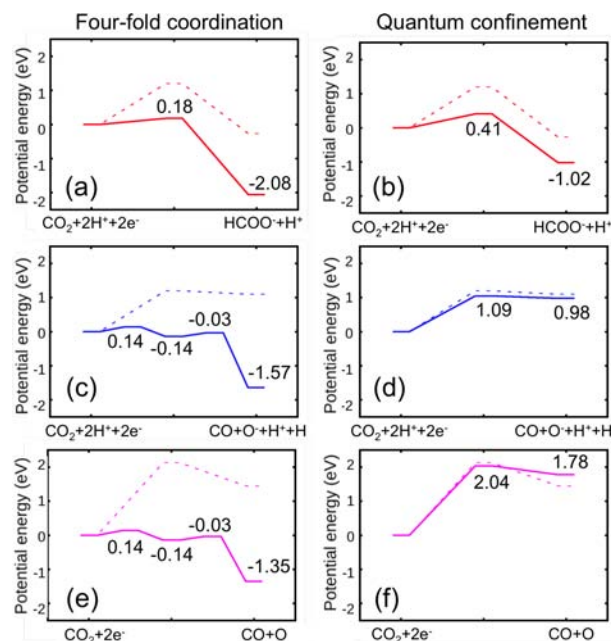


Figure 5. Reaction energetics change for three reaction mechanisms: (a,b) HCOO⁻ formation; (c,d) CO formation with protons; and (e,f) CO formation without protons. Left panels represent the four-fold coordination effect, and right panels represent the QC effect. Dotted lines indicate reaction energetics on the bulk surface.

factor along with the rate-determining energy barrier. Relative stabilities of these two states are summarized in Table 2. Note

Table 2. Energetic Stability Between HCOO⁻ and HCOOH at Surface^a

	HCOO ⁻ +H ⁺	HCOOH	ΔE (eV)
bulk	-0.27	-0.33	-0.06
QD	-1.68	-1.39	0.29
bulk Ti ₄	-2.08	-1.44	0.64
ribbon	-1.02	-0.95	0.07

^aEnergetics of each configuration are referenced to the initial physisorbed CO₂ state.

that both the four-fold titanium atom and the QC make HCOO⁻ state energetically more stable than HCOOH state undesirably. HCOO⁻ desorption is less preferable than HCOOH desorption for all cases in our calculation as expected,³³ and HCOOH formation can be thermodynamically unfavorable with the Ti₄ at surface and as the QC is enhanced in nanomaterials.

Our work shows insights into what aspects of nanostructures are important for CO₂ reduction on TiO₂ surfaces. The role of Ti₄ site and QC effect was elucidated using first-principles calculations. Our calculations show that there is a significant energy barrier associated with the first key CO₂ reduction step for all reaction mechanisms on the bulk anatase (101) surface. Such a large energy barrier is not observed on the QD surface. The role of Ti₄ atom and QC appears to vary significantly depending on reaction mechanism. Ti₄ atoms greatly help reduce the energy barrier for all the reaction mechanisms, while QC reduces the reaction barrier significantly only for HCOOH formation mechanism. At the same time, both Ti₄ atoms and QC undesirably tend to make the intermediate HCOO⁻ excessively stable with respect to HCOOH. One of the most

interesting findings is that Ti₄ atom makes the CO₂⁻ anion state stable with excess electrons at the surface. We stress that this enhanced stability of the CO₂⁻ state is the effect of the Ti₄ site and not directly of the oxygen vacancy created for the Ti₄. For instance, such stable CO₂⁻ anion state can be formed at Ti₄ substitutional site embedded in the inner wall of MCM-41 zeolite (Ti-MCM-41, see Figure S9), which has been employed experimentally.³⁴ In summary, our calculations show that CO formation mechanism is greatly facilitated by the presence of four-fold coordinated Ti atoms at surface.

Finally, we briefly comment on implications of our findings for photocatalytic CO₂ reduction with TiO₂ using solar energy. Since bulk TiO₂ is generally n-type semiconductor, the resulting band bending is not ideal because excess electrons are thermodynamically driven away from the surface even if Ti₄ atoms are present. Furthermore, the work by Cheng and Selloni¹⁴ indicates that oxygen vacancies might be thermodynamically more stable in subsurface than at the surface of the bulk anatase (101). Our work shows that one could instead take advantage of small TiO₂ nanoclusters or alternatively local Ti sites embedded in another host materials, such as MCM-41 in which significant Ti₄ atoms could be present. However, a straightforward usage of such TiO₂ nanomaterials might not be practical since further increases in the already large TiO₂ band gap (~3.2 eV) make them inefficient for utilizing solar photons. This could be overcome, for example, by doping the nanomaterials with sulfur atoms to reduce the energy gap significantly.³⁵ Since our study has shown the importance of Ti₄ and QC for CO₂ reduction, this work is likely to aid material design efforts for making CO₂ photocatalytic processes more efficient and selective. A systematic investigation of how TiO₂ nanomaterials of varying size and symmetry incorporate these effects for the catalytic activities is to be explored in a future work. The role of cocatalysts, such as palladium, has been shown to increase efficiency and product selectivity,⁶ and it is another important aspect that requires more investigation.

■ ASSOCIATED CONTENT

Ⓢ Supporting Information

Computational details and complete reference. This material is available free of charge via the Internet at <http://pubs.acs.org>.

■ AUTHOR INFORMATION

Corresponding Author

ykanai@unc.edu

Notes

The authors declare no competing financial interest.

■ ACKNOWLEDGMENTS

National Energy Research Scientific Computing Center, which is supported by the Office of Science of the U.S. DOE under contract no. DE-AC02-05CH11231, is acknowledged for providing computational resources. Some work was performed under the auspices of the U.S. DOE at Lawrence Livermore National Laboratory under contract no. DE-AC52-07NA27344.

■ REFERENCES

- (1) Fujishima, A.; Honda, K. *Nature* **1972**, *238*, 37.
- (2) Smestad, G. P.; Steinfeld, A. *Ind. Eng. Chem. Res.* **2012**, *51*, 11828.
- (3) Abe, R. *J. Photochem. Photobiol., C* **2010**, *11*, 179.
- (4) Inoue, T.; et al. *Nature* **1979**, *277*, 637.
- (5) Izumi, Y. *Coord. Chem. Rev.*, DOI: 10.1016/j.ccr.2012.04.018.
- (6) Yui, T.; et al. *ACS Appl. Mater. Interfaces* **2011**, *3*, 2594.
- (7) Xiong, L. B.; et al. *J. Nanomater.* **2011**, 831524.
- (8) Koci, K.; et al. *Appl. Catal., B* **2009**, *89*, 494.
- (9) Mori, K.; Yamashita, H.; Anpo, M. *RSC Advances* **2012**, *2*, 3165.
- (10) Lu, G. Q.; Linsebigler, A.; Yates, J. T. *J. Phys. Chem.* **1994**, *98*, 11733.
- (11) Herman, G. S.; et al. *J. Phys. Chem. B* **2003**, *107*, 2788.
- (12) Suriye, K.; Praserthdam, P.; Jongsomjit, B. *Appl. Surf. Sci.* **2007**, *253*, 3849.
- (13) Suriye, K.; et al. *Appl. Surf. Sci.* **2008**, *255*, 2759.
- (14) Cheng, H.; Selloni, A. *J. Chem. Phys.* **2009**, *131*, 054703.
- (15) Pan, J.; et al. *Angew. Chem., Int. Ed.* **2011**, *50*, 2133.
- (16) Liu, G.; et al. *Chem. Commun.* **2010**, 46, 755.
- (17) Vayssieres, L.; Persson, C.; Guo, J. H. *Appl. Phys. Lett.* **2011**, *99*, 183101.
- (18) Kong, M.; et al. *J. Am. Chem. Soc.* **2011**, *133*, 16414.
- (19) Wu, N.; et al. *J. Am. Chem. Soc.* **2010**, *132*, 6679.
- (20) Indrakanti, V. P.; Kubicki, J. D.; Schobert, H. H. *Energy Environ. Sci.* **2009**, *2*, 745.
- (21) Indrakanti, V. P.; Kubicki, J. D.; Schobert, H. H. *Fuel Process. Technol.* **2011**, *92*, 805.
- (22) He, H.; Zapol, P.; Curtiss, L. A. *J. Phys. Chem. C* **2010**, *114*, 21474.
- (23) Dey, G. R. *J. Nat. Gas Chem.* **2007**, *16*, 217.
- (24) Roy, S. C.; et al. *ACS Nano* **2010**, *4*, 1259.
- (25) Some indications in literature that hot carrier processes could be possible in some nanomaterials because of slow excited electron relaxation: Rajeshwar, K. In *Encyclopedia of Electrochemistry*; Licht, S., Ed.; Wiley-VCH: Germany, 2001.
- (26) Sun, C.; et al. *J. Mater. Chem.* **2010**, *20*, 10319.
- (27) Kohn, W.; Sham, L. J. *Phys. Rev.* **1965**, *140*, A1133.
- (28) Qu, Z. W.; Kroes, G. J. *J. Phys. Chem. C* **2007**, *111*, 16808.
- (29) Roduner, E. *Chem. Soc. Rev.* **2006**, *35*, 583.
- (30) Dimitrijevic, N. M.; et al. *J. Am. Chem. Soc.* **2011**, *133*, 3964.
- (31) Stanton, R. E.; McIver, J. W. *J. Am. Chem. Soc.* **1975**, *97*, 3632.
- (32) Lee, J.; Sorescu, D. C.; Deng, X. *J. Am. Chem. Soc.* **2011**, *133*, 10066.
- (33) DFT calculations show that desorption energy of HCOO⁻ (2.06/2.49/3.54/1.86 eV for bulk/QD/bulk-Ti₄/ribbon) is much larger than that of HCOOH (0.40/0.46/0.66/0.48 eV).
- (34) Anpo, M.; et al. *Catal. Today* **1998**, *44*, 327.
- (35) Umezawa, N.; et al. *Appl. Phys. Lett.* **2008**, *92*, 041104.